THE JOURNAL OF BIOLOGICAL CHEMISTRY VOL. 288, NO. 15, pp. 10548–10557, April 12, 2013

Nicotinamide Inhibits the Lysosomal Cathepsin b-like Protease and Kills African Trypanosomes*

Received for publication, December 30, 2012, and in revised form, February 25, 2013 Published, JBC Papers in Press, February 26, 2013, DOI 10.1074/jbc.M112.449207

Juan D. Unciti-Broceta[‡§], José Maceira[‡§], Sonia Morales[‡§], Angélica García-Pérez[‡§], Manuel E. Muñóz-Torres[¶], and Jose A. Garcia-Salcedo[‡§1]

From the [‡]Unidad de Enfermedades Infecciosas, [¶]Unidad de Metabolismo Óseo, Instituto de Investigación Biosanitaria de Granada (IBIG) , Av. Dr. Olóriz 16, 18012 Granada, Granada, Spain and the [§]Instituto de Parasitología y Biomedicina "López Neyra" (IPBLN-CSIC), Av. del Conocimiento s/n, 18016 Armilla, Spain

Background: Nicotinamide is a soluble compound of the vitamin B_3 group with antimicrobial activity.
Results: Nicotinamide causes disruption of the lysosome and inhibits the cathepsin b-like enzyme, an essential lysosomal protease in trypanosomatids.
Conclusion: Nicotinamide kills African trypanosomes by targeting the cathepsin b-like protease.
Significance: These results demonstrate for the first time the inhibitory effect of nicotinamide on a protease.

Nicotinamide, a soluble compound of the vitamin B_3 group, has antimicrobial activity against several microorganisms ranging from viruses to parasite protozoans. However, the mode of action of this antimicrobial activity is unknown. Here, we investigate the trypanocidal activity of nicotinamide on *Trypanosoma brucei*, the causative agent of African trypanosomiasis. Incubation of trypanosomes with nicotinamide causes deleterious defects in endocytic traffic, disruption of the lysosome, failure of cytokinesis, and, ultimately, cell death. At the same concentrations there was no effect on a cultured mammalian cell line. The effects on endocytosis and vesicle traffic were visible within 3 h and can be attributed to inhibition of lysosomal cathepsin b-like protease activity. The inhibitory effect of nicotinamide was confirmed by a direct activity assay of recombinant cathepsin b-like protein. Taken together, these data demonstrate that inhibition of the lysosomal protease cathepsin b-like blocks endocytosis, causing cell death. In addition, these results demonstrate for the first time the inhibitory effect of nicotinamide on a protease.

Nicotinamide, the amide form of vitamin B_3 (niacin), is used to synthesize NAD through the salvage pathway once taken up by cells (1, 2). In addition, nicotinamide is also a known inhibitor of mono- and poly-ADP-ribosyltransferases such as poly ADP-ribosyltransferase and sirtuin proteins. There is extensive literature that describes the beneficial cellular effects of nicotinamide on mammalian cells. For example, nicotinamide promotes maturation of fetal cells (3) and induces proliferation and differentiation of embryonic stem cells to yield insulin-producing cells (4). It also protects brain cells from oxidative damage caused by reperfusion after ischemic infarction (5–7) and prevents injury of pancreatic islet cells during free radical exposure (8). Moreover, nicotinamide has also been shown to exhibit cytoprotective qualities in immune system dysfunction, aging-associated diseases, and diabetes (9).

Although nicotinamide has also been shown to be active against a variety of pathogens and viruses, *e.g. Mycobacterium tuberculosis* (10), *Leishmania* (11, 12), *Plasmodium* (13), *Trypanosoma cruzi* (14) and HIV (10, 15), the mechanism of this activity has not been elucidated.

African trypanosomiasis is a vector-borne disease that occurs in impoverished rural parts of sub-Saharan Africa, where millions of people are at risk of infection (16). It is caused by the flagellated protozoa *Trypanosoma brucei* and transmitted by tsetse flies of the genus *Glossina*. The subspecies *Trypanosoma brucei gambiense* and *Trypanosoma brucei rhodesiense* cause human African trypanosomiasis, also called sleeping sickness. In addition, the parasite infects domestic animals, contributing to Nagana, a devasting disease of livestock in Africa.

Proteases are ubiquitous in nature and, through degradation of proteins, regulate and coordinate a large number of cellular processes. Therefore, they are essential to many organisms. Among them, serine proteases are the most abundant in mammalian cells. In contrast, parasitic organisms commonly rely on cysteine proteases of the Clan CA family (17). In addition to their housekeeping function, cysteine proteases are closely associated to processes that support parasitism, such as the digestion of host components. Thus, they are considered as potentially effective drug targets for the treatment of many parasitic diseases (18). Bloodstream *T. brucei* parasites express two cysteine proteases of the papain family: rhodesain (brucipain, trypanopain), a cathepsin L-like enzyme and TbCatB[2], a cathepsin b-like protease. Treatment of parasites in culture with the cysteine protease inhibitor benzyloxycarbonyl-phenylalanyl-alanyl diazomethane was lethal to *T. brucei in vitro* (19).

* This work was supported by Plan Nacional de Investigación (Ministerio de Economía y Competitividad, Spain) Grant SAF2011-30528 (to J. A. G. S.) and European Union Grant FP7-HEALTH-2007-B-2.3.4-1.223048, NANOTRYP (to J. A. G. S.).
[1] To whom correspondence should be addressed: Instituto de Parasitología y Biomedicina "López Neyra" (IPBLN-C.S.I.C.) 18100 Granada, Spain. Tel.: 34-958-181638; Fax: 34-958-181632; E-mail: jagarciasalcedo@ipb.csic.es.

[2] The abbreviations used are: TbCatB, *Trypanosoma brucei* cathepsin b-like protease; PFA, paraformaldehyde; PI, propidium iodide; Z-Arg-Arg-AMC, Z-arginine-arginine 7-amido-4-methylcoumarin hydrochloride; K, kinetoplast(s); N, nucleus/nuclei

Parasites treated with this inhibitor exhibited altered cell morphology, were unable to undergo cytokinesis, and were defective in host protein degradation (20). Significantly, a study demonstrated that specific knockdown of TbCatB expression by RNAi was lethal in *T. brucei* and produced phenotypic defects similar to those seen with the inhibitor (21). Indeed, knockdown of TbCatB *in vivo* was able to rescue mice from a lethal *T. brucei* infection (22). In contrast, knockdown of rhodesain, the cathepsin L-like enzyme, had no deleterious effects on the parasites (22). Taken together, these results indicate that one of the two cysteine proteases of the Clan CA family in *T. brucei*, the cathepsin b-like enzyme, is the key target of the protease inhibitor and represents a prime target for development of anti-trypanosome therapies.

This study describes the trypanocidal activity of nicotinamide and establishes the basis for this activity. Treatment with nicotinamide produced early defects in endocytosis and cytokinesis, resulting in parasite death. These cellular effects can be linked to the finding that nicotinamide was found to be a inhibitor of the trypanosome cathepsin b-like activity *in vivo* and *in vitro*.

EXPERIMENTAL PROCEDURES

Cell Culture—Bloodstream forms of *T. brucei* (wild type 427) were grown in axenic culture at 37 °C and 5% CO_2 in HMI-9 medium (GIBCO) supplemented with 10% heat-inactivated FBS (Invitrogen). The 293T human renal epithelial cell line was grown in Dulbecco's modified Eagle's medium (or minimum essential medium) (Invitrogen) supplemented with 10% heat-inactivated FBS (Invitrogen) in axenic culture at 37 °C and 5% CO_2. Human umbilical vein endothelial cells (Lonza) were cultured in EBM-2 culture medium supplemented with EGM-2 SingleQuots (FBS, hydrocortisone, heparin-binding growth factor/basic fibroblast growth factor, vascular endothelial growth factor, human recombinant insulin-like growth factor, ascorbic acid, human epidermal growth factor, GA-1000, heparin) (Lonza) on flasks coated with 1% gelatin. Primary human foreskin fibroblasts were culture in Iscove's modified Dulbecco's medium (Invitrogen) supplemented with 10% heat-inactivated FBS (Invitrogen) at 37 °C and 5% CO_2.

Trypanotoxicity Assays—The sensitivity of trypanosomes to nicotinamide susceptibility was assessed using the sodium resarzurin protocol with some modifications (23). Exponentially growing parasites were harvested and prepared at an initial density of 2 × 105 trypanosomes/ml. Each well of a 96-well tissue culture plate containing 50 μl from serial doubling dilutions of nicotinamide was inoculated with 50 μl of trypanosome culture, with the exception of two rows, which received medium only. Eleven different final concentrations of nicotinamide, ranging from 0.4–400 mM, were tested in the assay. Parasites were incubated for 20 h at 37 °C and 5% CO_2. Then, 20 μl of 0.5 mM sodium resarzurin dye (Sigma) was added to each well, and the plate was incubated for a further 4 h. The reaction was stopped by adding 50 μl of 3% SDS and then read on a Tecan Infinite F200 reader (Tecan Austria GmbH, Austria) using excitation emission wavelengths of 535 nm and 590 nm (24). Each concentration point was assayed in six replicates, and experiments were repeated three times. The IC_{50} value was calculated using GraphPad Prism5 software and defined as the concentration of drug required to diminish the fluorescence output by 50%. The same protocol was performed in all human cell lines. The cells were seeded at an initial density of 1×10^5 cells/ml 24 h before nicotinamide addition.

The effects of nicotinamide on cellular morphology and cell cycle progression were analyzed by fluorescence and differential interference contrast microscopy. At various times after addition of nicotinamide, parasites were fixed in 4% PFA. Then trypanosomes were washed with PBS three times, spread on poly-L-lysine-coated slides and mounted in DAPI-containing Vectashield medium (Vector Laboratories, Burlingame, CA). Image acquisition was performed with an inverted Olympus IX81 microscope equipped with a charge-coupled device camera (Orca charge-coupled device, Hamamatsu), and Cell R IX81 software. Two hundred cells were counted at each time point. Parasites were classified according to the number of nuclei (N) and kinetoplasts (K).

Analysis of Cell Cycle and DNA Degradation by FACS—DNA content was assed as described previously (25). Samples (2.5×10^6 cells) of nicotinamide-treated and untreated *T. brucei* bloodstream forms were fixed in 900 μl of ice-cold ethanol (70%), incubated on ice for at least 5 min, and washed with PBS and incubated PI staining solution (PBS containing 40 μg/ml PI and 100 μg/ml ribonuclease A) for at least 30 min. The analysis was performed with a FACSCalibur flow cytometer (BD Biosciences). An estimation of the number of cells at the G_1, S, and G_2/M phases of the cell cycle was performed using BD Biosciences CellQuest software. The relative percentage of dead cells was quantified on the basis of the sub-G_1 subpopulation. Dot plots were performed using FlowJo software. The experiment was performed in triplicate and repeated at least three times.

Transmission Electron Microscopy—Trypanosomes were fixed and processed for transmission electron microscopy as described previously (26). Briefly, bloodstream trypanosomes (10^8 cells) were fixed in 2.5% (v/v) glutaraldehyde, 2% PFA in 0.1 M sodium cacodylate buffer (pH 7.2) for 24 h at 4 °C and post-fixed in 2% osmium tetroxide in the same buffer. Then the samples were stained with 2% uranyl acetate for 2 h in the dark. After dehydration using increasing ethanol concentrations and clearing in propylene oxide, the samples were embedded in Embed 812 resin for 2 h and left to polymerize for 4 days at 60 °C. Ultrathin sections (50–70 nm thick) were generated and transferred to Formvar carbon-coated copper grids by using a Leica Ultracut R ultramicrotome and stained with uranyl acetate and lead citrate. Observations were made on a TEM Libra 120 plus (Zeiss), and images were captured with a slow-scan charge-coupled device 2K × K MegaView II camera and processed with AnalySIS and Adobe softwares.

Staining of Acidic Organelles—Bloodstream forms (10^6 cells) treated with nicotinamide for different periods of time were incubated for 10 min at 37 °C in HMI-9 complete medium containing 100 nM LysoTracker Green DND-26 acidotropic dye (Invitrogen). Then the parasites were washed and resuspended in PBS. The fluorescence signal was measured by flow cytometry in a FACSCalibur flow cytometer (excitation at 488 nm and emission between 515 and 545 nm), and the data were analyzed with BD CellQuest software.

Endocytosis Assays—Endocytosis assays were performed with FITC-labeled tomato lectin as described previously (27). Briefly, nicotinamide-treated and untreated bloodstream trypanosomes (10^7 cells) were washed with PBS, centrifuged at 7000 rpm, and resuspended in 1 ml of free serum HMI-9 supplemented with 10 mg/ml of BSA containing tomato lectin-FITC conjugate (Sigma) at 20 μg/ml. Cells were incubated for 60 min at 37 °C and then washed with PBS supplemented with 1% of FBS. Finally, cells were fixed in 4% PFA in PBS and analyzed by FACSCalibur using CellQuest software.

Fluid-phase endocytosis was performed using FITC-dextran (average molecular mass, 10,000, FD10S, Sigma). Nicotinamide-treated bloodstream trypanosomes were incubated with nicotinamide at 37 °C for 3 or 6 h and then washed and resuspended in 0.5% BSA/HMI-9 medium with FITC-dextran at 0.5 mg/ml. Then cells were incubated for 1 h at 37 °C and fixed in 4% PFA. Fixed parasites were analyzed mounted onto poly-L-lysine slides in DAPI-containing Vectashield medium (Vector Laboratories) and processed for immunofluorescence microscopy analysis. Untreated cells were processed in the same manner.

Indirect Immunofluorescence Microscopy—Immunofluorescence was performed as described previously by Landeira *et al.* (28), with some modifications. Parasites were fixed in 4% PFA and permeabilized with washing solution (0.2% Triton X-100 in PBS buffer). Cells were then blocked with blocking solution (1% BSA in washing solution) and incubated with the corresponding primary antibodies against p67 protein (mouse anti-trypanosome) provided by J. D. Bangs (University of Wisconsin-Madison, Madison, WI). Then, the cells were washed and incubated with Alexa Fluor 488-labeled goat anti-mouse (Invitrogen). Finally, trypanosomes were washed with PBS three times, spread on poly-L-lysine-coated slides, and mounted in DAPI-containing Vectashield medium (Vector Laboratories). Image acquisition was performed with an inverted Olympus IX81 microscope equipped with a charge-coupled device camera (Orca charge-coupled device; Hamamatsu) and Cell R IX81 software. Deconvolution of three-dimensional images was performed using Huygens Essential software (version 2.9, Scientific Volume Imaging).

Cloning, Expression, and Purification of Recombinant TbCatB in Pichia pastoris—The TbCatB plasmid was provided by Dr. Zachary B. Mackey (University of California). Methods for TbCatB cloning and expression of the recombinant TbCatB in *P. pastoris* have been described previously (29, 30). After 48 h of methanol induction, *P. pastoris* cultures were centrifuged at 3000 × *g* for 10 min, and the resulting supernatant containing recombinant TbCatB was lyophilized. The crude lyophilized protein was resuspended in 10% of the original volume in 50 mM sodium citrate buffer (pH 5.5) and desalted using PD-10 columns (GE Healthcare/Amersham Biosciences) by equilibrating in the same buffer. The solution was loaded onto a Mono Q 5/50 anion exchange column using an Akta Purifier-900 chromatography system (both GE Healthcare/Amersham Biosciences). A 50 mM 2-(*N*-morpholino) ethanesulfonic acid (pH 6.5) buffer was used for column equilibration, sample loading, and protein elution with a flow rate of 1 ml/min. Protein was eluted with a linear gradient of 0–1 M sodium chloride concentration over 20 min. Fractions of 0.5 ml were collected and subsequently checked for purity by Coomassie-staining SDS-PAGE gel.

Protease Activity Assay—Protease activity on total cell extracts was measured using the fluorogenic peptide substrate Z-Arg-Arg-AMC (Bachem I-1135), which is cleaved by the protease to release free AMC. Briefly, *T. brucei* bloodstream forms (10^7 cells) were centrifuged, washed once in PBS containing 1% glucose and resuspended in a buffer containing 150 mM sodium phosphate, 200 mM NaCl, 5 mM EDTA and 5 mM DTT, pH 6.0. Then, CHAPS at final concentration of 1% was added and incubated on ice 1 h (31). The lysate was cleared by centrifugation at 13000 rpm for 15 min at 4 °C. A volume of 100 μl of supernatant containing the enzyme was preactivated in 1.8 ml of the same buffer (without CHAPS) for 10 min at 37 °C and the reaction started by adding Z-Arg-Arg-AMC substrate at 10 μM final concentration. The release of AMC was measured at an excitation and emission wavelength of 350 nm and 460 nm, respectively, in a luminescence spectrometer (Amico-Bowman). The assay was performed three times. The same protocol was conducted to obtain total cellular extract from *Leishmania donovani* and *T. cruzi*.

Protease Activity of Recombinant TbCatB—TbCatB activity was measured as follows. Each well of a 96-well flat-bottom plate containing 50 μl of serial doubling dilutions of nicotinamide in sodium citrate buffer (50 mM (pH 5.5)) with 4 mM DTT was inoculated with 50 μl of recombinant TbCatB at 2 ng/μl in the same buffer, with the exception of two blank rows, which received only buffer. Ten different concentrations of nicotinamide (ranging from 25 μM to 25 mM) were tested. The plate was preincubated at 25 °C for 10 min. Following the preincubation period, 100 μl of Z-Arg-Arg-AMC substrate (20 μM, prepared in the same buffer) was added to the enzyme solution to give a final concentration of 10 μM and a final volume of 200 μl. Hydrolysis was measured every 1 minute for 30 min at 25 °C using an automated microtiter plate spectrofluorimeter (PerkinElmer Life Sciences). Excitation and emission wavelengths were 350 and 460 nm, respectively. Each test was set up in six replicates/concentration and repeated three times. The same experiment was performed using different final concentrations of substrate (0.2, 3.2, 6.4, 12.8, and 25.6 μM) to determine the inhibition constant (K_i). The kinetic data were analyzed fitted to the appropriate equation using GraphPad Prism version 5.00 for Windows (GraphPad Software, San Diego, CA).

Kinetics of Transferrin Uptake and Degradation—Bloodstream forms were incubated in HMI-9 complete medium for 10 min at 37 °C in the presence of nicotinamide. Non-treated parasites, as a control, were assessed at the same conditions. Afterward, the parasites were washed twice and resuspended in prewarmed trypanosome dilution buffer (5 mM KCl, 80 mM NaCl, 1 mM $MgSO_4$, 20 mM Na_2HPO_4, 2 mM NaH_2PO_4, 20 mM glucose (pH 7.4)) at a density of 8×10^6 parasites/ml. Transferrin from human serum (Alexa Fluor 488-conjugated, Molecular Probes) was added to the suspension, and the parasites were incubated at 37 °C. At different times, samples of 250 μl were taken and fixed in 250 μl of ice-cold 8% PFA. The fluorescence was measured by flow cytometry in a FACSCalibur flow cytometer (excitation at 495 nm and emission 519 nm). Relative fluo-

rescence was calculated with respect to the fluorescence value at time zero. Data are the means ± S.D. from three independent experiments.

Phosphatidylserine Exposure Assay—Control and nicotinamide-treated *T. brucei* bloodstream forms (2–5 × 10^5 cells/ml) were washed with annexin V binding buffer (10 mM HEPES, 140 mM NaCl, 3.3 mM $CaCl_2$) and resuspended in 100 μl of this buffer. 5 μl of commercially available annexin V-FITC solution (Bender MedSystems) was added to each sample, followed by incubation for 15 min in the dark at room temperature. After a final wash, the pellet was resuspended in annexin V binding buffer plus 10 μl of PI (20 μg/ml). Stained samples were immediately analyzed by flow cytometry using a FACSCalibur flow cytometer. Data were analyzed with FlowJo software.

RESULTS

Nicotinamide Inhibits Growth and Induces Morphological Changes in Bloodstream Forms of T. brucei—The trypanocidal effect of nicotinamide on *T. brucei* bloodstream cells was evaluated by using a sodium resarzurin assay. Nicotinamide showed a dose-dependent effect on trypanosome viability, and an IC_{50} and 95% inhibitory concentration (IC_{95}) of 9.86 ± 0.15 mM and 49.53 ± 2.75 mM, respectively (mean ± S.D. of three separate determinations) were obtained (Fig. 1*A*). This concentration range had no effect on the growth of a 293T human renal epithelial cell line, and the IC_{50} determined for this human cell line was almost 20 times higher (175.67 ± 4.45 mM) than that observed for trypanosomes (Fig. 1*A*). Moreover, in two types of primary human cells, umbilical vein endothelial cells and human foreskin fibroblast, the IC_{50} was 61.51 ± 2.42 and 68.07 ± 1.79, respectively, about 7-fold higher than in *T. brucei*. This result was in agreement with previous observations that concentrations of nicotinamide in the micromolar range have no deleterious effects on mammalian cell viability (32–33), in contrast to that observed in *T. brucei* bloodstream cells. In fact, this is the usual range of concentrations for other uses of nicotinamide (3–9). The nicotinamide IC_{95} (50 mM) was chosen to carry out the rest of this study.

The effect of nicotinamide on trypanosome morphology was investigated by phase contrast microscopy (Fig. 1*B*). Incubation with nicotinamide resulted in an enlargement/swelling of the posterior end of the cell that was progressive with time (Fig. 1*B*). Within 6 h, about 40% of the cells exhibited an abnormal morphology that correlated with the appearance of a phase light vacuole in the posterior region of the cell. After an incubation of 24 h, most of the cells were grossly distorted and no longer possessed the typical long, slender morphology (Fig. 1*C*).

Nicotinamide Causes Cytokinesis Defects and Cell Cycle Arrest at G_2 Phase—The progression of African trypanosomes through the different phases of the cell cycle can be monitored by the configuration of the kinetoplast (K) and the nucleus (N). Cell containing a single nucleus and kinetoplast (1N1K) are in G_1 phase, and an arrangement of two kinetoplasts and one nucleus (2K1N) represents cells in S phase and G_2/mitosis, whereas postmitotic cells contain two nuclei and two kinetoplasts (2K2N). Analysis of the K/N ratio of cells incubated with nicotinamide revealed a time-dependent decrease in the percentage of cells in G_1 phase and an accumulation of postmitotic

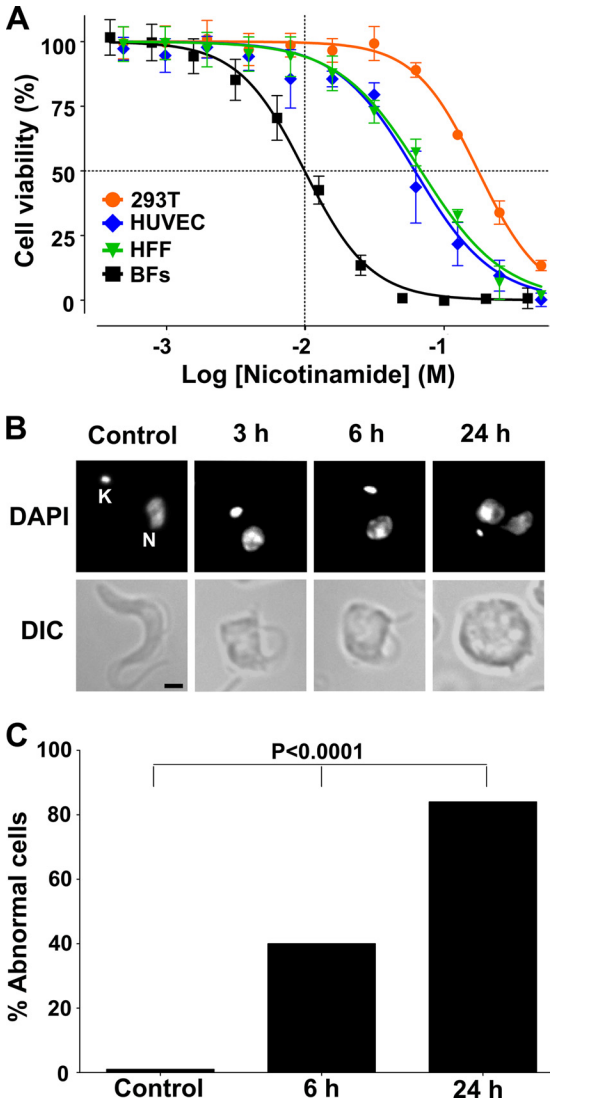

FIGURE 1. **Effect of nicotinamide on cell viability and morphology.** *A*, curve dose response (viability percent *versus* nicotinamide concentration). The IC_{50} value was determined by log(inhibitor) *versus* normalized response − variable slope using GraphPad software. *293T*, human renal epithelial cell line; *HUVEC*, human umbilical vein endothelial cells; *HFF*, human foreskin fibroblast; *BFs*, *T. brucei* bloodstream forms. *B*, bloodstream trypanosomes incubated with nicotinamide for 0, 3, and 6 h. DAPI-stained parasites were observed by fluorescence microscopy (*top line*) and differential interference contrast (*DIC*) (*bottom line*). *C*, percentage of abnormal cells. Statistical significance, $p < 0.0001$, was determined by a Chi-square test using GraphPad software.

cells and multinucleate cells (Fig. 2*A*). The percentage of 1K1N cells present in the population decreased from ~86% to 38% after 24-h incubation with nicotinamide. There was a concomitant 4-fold increase in the number of 2K2N cells (from ~4 to 15%) during this time. Simultaneously, there was a very significant increase in the number of aberrant cells containing several nuclei and kinetoplasts from less than 2% to more than 17%. Taken together, these findings were consistent with the view that incubation with nicotinamide caused an arrest in cytokinesis in cells after completing several rounds of DNA synthesis and mitosis.

To further analyze the effect of nicotinamide on cell cycle progression, the DNA content of cells incubated with nicotin-

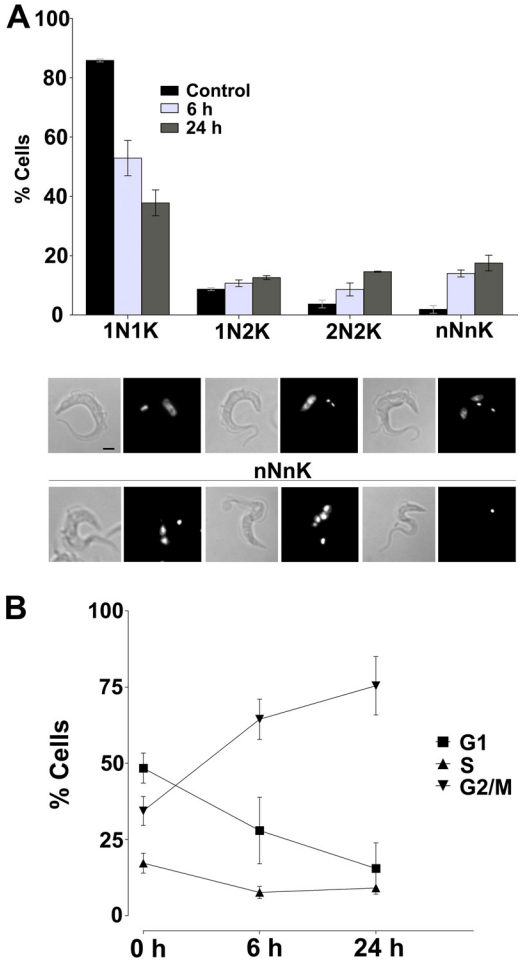

FIGURE 2. **Effect of nicotinamide on the cell cycle of *T. brucei*.** *A*, quantification of cells with different number of nuclei and kinetoplasts after exposure to nicotinamide for 6 and 24 h. The results are expressed as mean ± S.D. of three experiments. *Bottom panel*, *top row*, three normal cell types (*1N1K*, *1N2K*, and *2N2K*). *Bottom row*, three examples of aberrant cells (*nNnK*). *B*, FACS analysis of the cell cycle-type population after 0, 6, and 24 h of exposure to nicotinamide. Percentages were determined using CellQuest software excluding the $SubG_1$ population. Data are mean ± S.D. from three independent experiments.

amide was assessed by flow cytometry. In the case of untreated trypanosomes, the distribution of cells, as the percentage of the total live cell population, at the different phases of the cell cycle presented a classical cell cycle distribution for bloodstream trypanosomes. There was a major G_1 population (~50%), followed by large a G_2/M population of ~34% and a small S phase associated with active DNA synthesis (~17%) (Fig. 2*B*). Significantly, incubation with nicotinamide resulted in a major shift in the live cell population, with a virtual doubling of the number of cells in G_2/M phase to ~75% and a concomitant 50% decrease in G_1 phase cells after 24 h (Fig. 2*B*). Together, these results indicate that incubation with nicotinamide (50 mM) initially causes cell cycle arrest at G_2/M phase and interferes with cytokinesis of bloodstream forms of *T. brucei*.

Nicotinamide Inhibits Endocytosis—Phase contrast microscopy demonstrated that incubation with nicotinamide caused enlargement and swelling of the posterior region of the cell that is associated with endocytic traffic. Transmission electron microscopy was used to investigate these morphological changes at the ultrastructural level. Significantly, in many sections taken after 3–6 h of nicotinamide treatment, the flagellar pocket was grossly enlarged, as revealed by the relative size of the flagellum compared with the lumen of the pocket (Fig. 3*A*). Furthermore, multiple flagella within the flagellar pocket were also observed in some sections, consistent with a failure to complete the process of cell division (data not shown). The enlargement of the flagellar pocket observed in electron micrographs correlated well with the presence of the enlarged vacuole observed by phase contrast microscopy. Moreover, an accumulation of vesicles and tubular structures close to the pocket was observed in sections of treated cells, and these structures appeared to increase in number and size with time. During this time (6 h), there was also an increase in the accumulation of the acidotropic dye LysoTracker Green, which indicated an increase in the number of intracellular acidic organelles (Fig. 3*B*).

In bloodstream trypanosomes, enlarged flagellar pocket morphology, known as the "big eye" phenotype, is associated with the inhibition of the endocytosis process (34). The effect of nicotinamide on endocytosis was directly studied by FACS analysis of the uptake of FITC-labeled tomato lectin (Fig. 3*C*). Lectin internalization, represented by the amount of intracellular fluorescent signal, was clearly diminished after trypanosome incubation with nicotinamide. We also tested whether nicotinamide affects fluid phase endocytosis by measuring FITC-dextran uptake by bloodstream trypanosomes. A similar decrease in the uptake of FITC-dextran was observed in trypanosomes incubated with nicotinamide (Fig. 3*D*). Taken together, these data indicate that at midterm, nicotinamide treatment interferes with the endocytosis process in bloodstream forms of *T. brucei*.

Nicotinamide Induces Lysosome Disruption and Cathepsin b-like Protease Inhibition—To identify perturbations in vesicle trafficking, the distribution of a lysosomal marker, p67, a lysosomal type I membrane glycoprotein (35), was investigated using immunofluorescence microscopy. In untreated bloodstream trypanosomes, anti-p67 antibodies revealed a highly polarized distribution of the protein that was concentrated as a discrete spot located between the kinetoplast and the nucleus (Fig. 4*A*). In contrast, in nicotinamide-treated cells, p67 distribution was significantly less polarized, and several smaller spots of lower fluorescence intensity were observed (Fig. 4*A*). These results indicate that incubation with nicotinamide results in disruption of the lysosome integrity. Therefore, the effect of nicotinamide on lysosomal function was assessed by measuring protease activity in total cellular extracts from control and treated cells using the fluorogenic peptide substrate Z-Arg-Arg-AMC. Significantly, nicotinamide had an inhibitory effect on the cellular cathepsin b-like activity, which decreased by ~75% with respect to control cells within 1 min of addition of nicotinamide (Fig. 4*B*). After 30 min, the total activity was ~10% of the control levels and then remained constant. This result suggests that trypanosomes contain a nicotinamide-sensitive protease activity that represents the bulk of the cathepsin b-like activity and a smaller nicotinamide-insensitive activity.

Cathepsin b-like is a lysosomal protease responsible for degradation of host-derived growth factors, such as transferrin, in

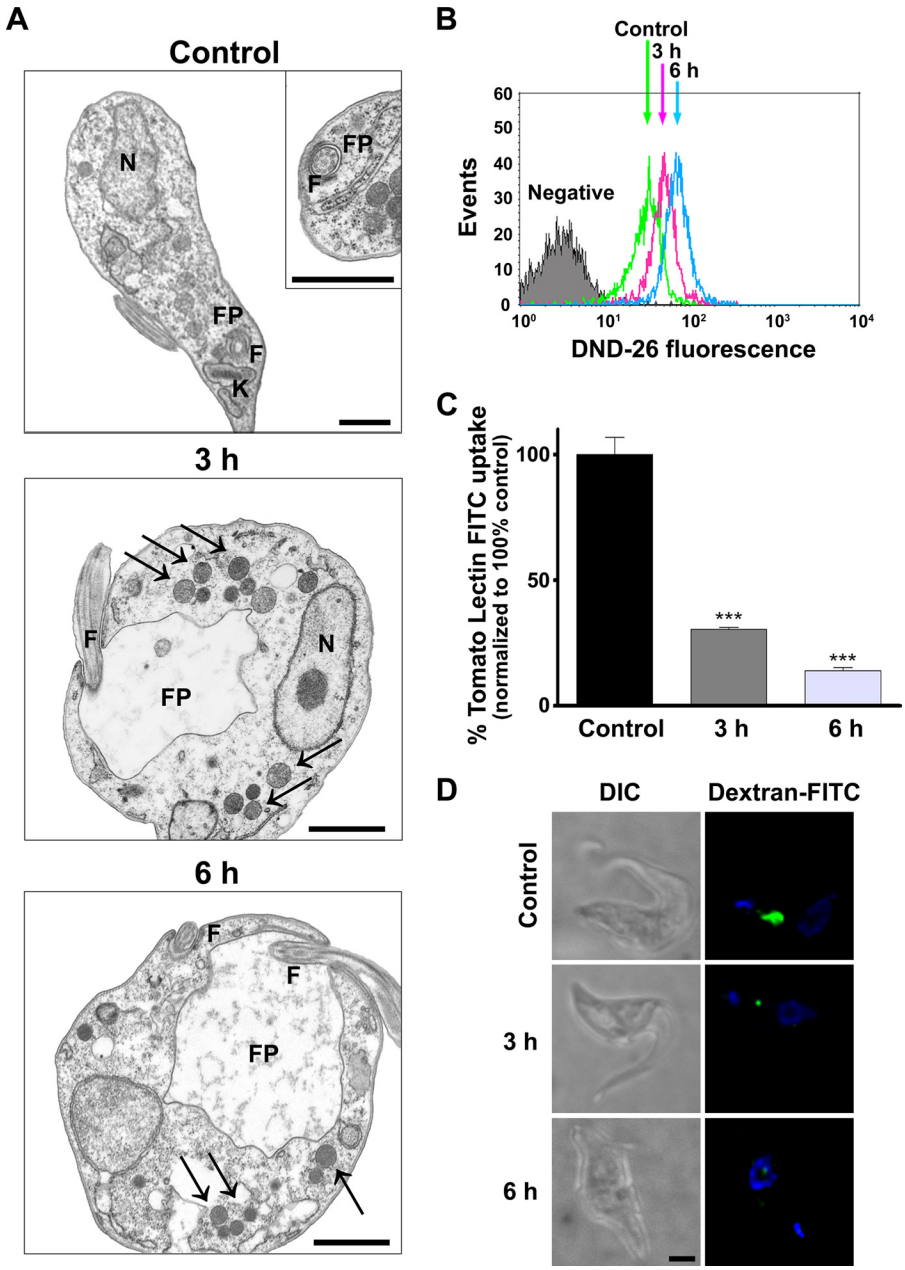

FIGURE 3. **Nicotinamide inhibits endocytosis in *T. brucei*.** *A*, transmission electronic microscopy analysis of bloodstream forms after nicotinamide treatment. *F*, flagellum; *FP*, flagellar pocket. *Black arrows* indicate vesicles and tubular structures. *Scale bars* = 1 μm. *B*, FACS analysis of acid organelle quantification after nicotinamide exposure measuring mean fluorescence intensity of the acidotropic dye LysoTracker Green (*DND-26*). *C*, FACS analysis of tomato lectin-FITC uptake. Statistical significance was determined by Bonferroni's multiple comparison test between treated *versus* control cells. ***, $p < 0.001$. *D*, dextran-FITC accumulation. Untreated trypanosomes as well as nicotinamide-pretreated parasites were incubated for 1 h with dextran-FITC particles, fixed, and analyzed by fluorescence microscopy. *DIC*, differential interference contrast; *green*, dextran-FITC; *blue*, DAPI. *Scale bar* = 1 μm.

the bloodstream form of *T. brucei*. Transferrin is the unique source of iron for the parasite and is internalized from the host through receptor-mediated endocytosis. The host transferrin is then rapidly degraded in the lysosome. To investigate the effect of nicotinamide on transferrin degradation, bloodstream forms were incubated with Alexa Fluor 488-labeled transferrin, and transferrin uptake was analyzed by flow cytometry (Fig. 4*C*). In untreated cells, an increase in the cell-associated fluorescent signal was observed within the first 5 min, which then declined slightly, indicating an initial uptake of Alexa Fluor 488-transferrin followed by a rapid protein degradation. When the assay was performed after nicotinamide treatment, a slower but continuous increase in the fluorescent signal was observed over the time course experiment, suggesting an inhibitory effect on both transferrin uptake and degradation.

Finally, to determine whether nicotinamide is an inhibitor of *T. brucei* cathepsin b-like protease (TbCatB), recombinant TbCatB was expressed and purified. Expression of TbCatB in *P. pastoris* led to secretion of a 42-kDa protein corresponding to the zymogen form of the enzyme (Fig. 4*D*). Protease activity was monitored using the fluorogenic peptide substrate Z-Arg-Arg-AMC at different concentrations of nicotinamide. As shown in Fig. 4*E*, recombinant TbCatB protease activity was completely inhibited at 25 mM.

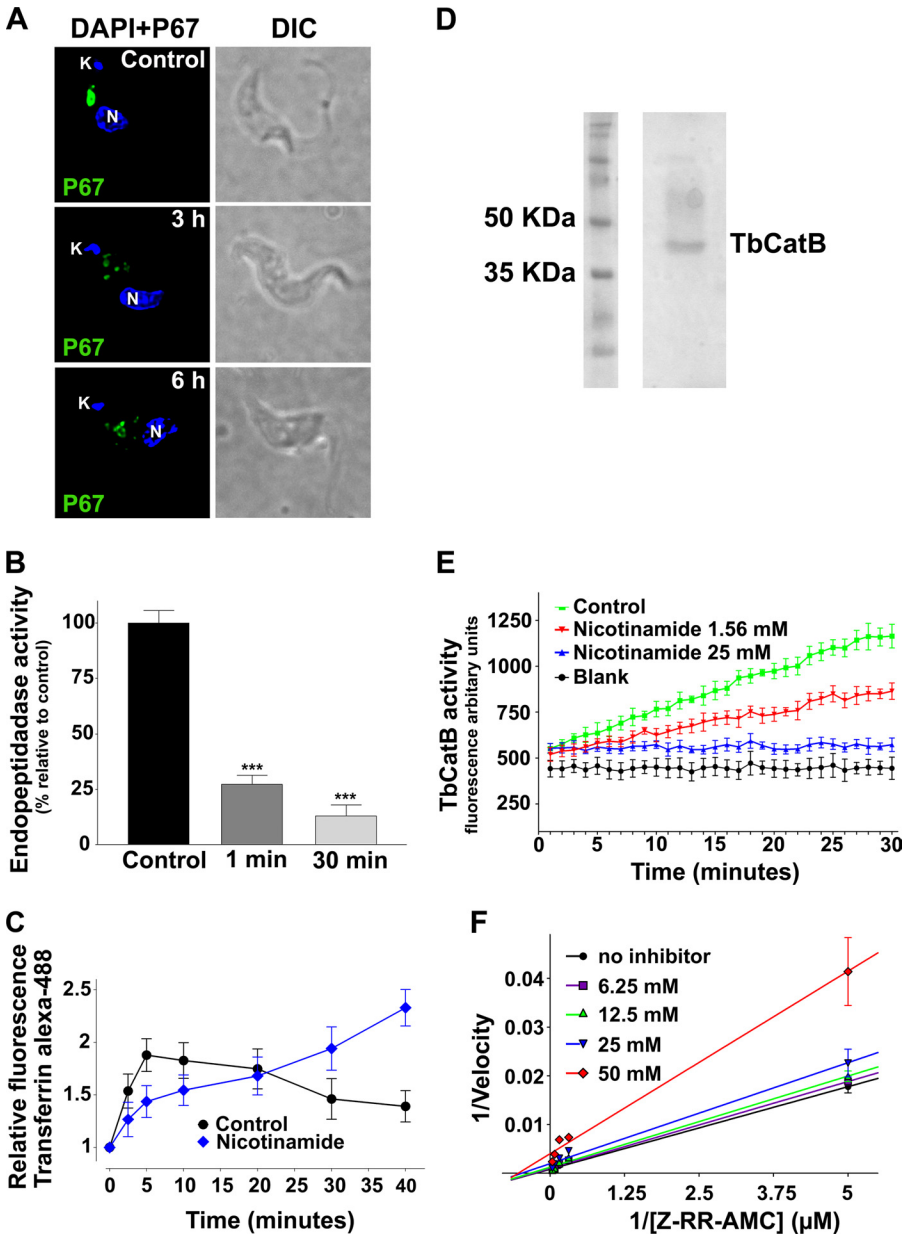

FIGURE 4. **Nicotinamide affects lysosome morphology and function.** *A*, localization of p67. *Left panel*, *blue*, DAPI; *green*, p67. *Right panel*, differential interference contrast (*DIC*). *B*, cathepsin b-like activity in parasite extracts using the fluorogenic peptide Z-Arg-Arg-AMC substrate. Values are mean ± S.D. of three different experiments. Statistical significance was determined by Bonferroni's multiples comparison test, treated *versus* control. ***, $p < 0.001$. *C*, FACS analysis of transferrin-Alexa Fluor 488 uptake. Results are mean ± S.E. from three independent experiments. *D*, SDS-PAGE gel of purified recombinant TbCatB visualized by Coomassie stain. *E*, purified recombinant TbCatB activity was monitored using the release of AMC after hydrolysis of the specific substrate Z-Arg-Arg-AMC. Control, untreated (*green*); nicotinamide, 1.56 mM (*red*), 25 mM (*blue*); blank (*black*). Data are mean ± S.D. from six replicates in three different experiments. *F*, linear regression of a Lineweaver-Burk double-reciprocal plot depicting the non-competitive inhibitory activity of nicotinamide on recombinant TbCatB. All data represent the mean of at least three replicates in three different experiments (*error bars* indicate S.E.).

The kinetic properties of the recombinant TbCatB were determined using a stopped assay. Protease activity was determined at a fixed time point (30 min), over a range of Z-Arg-Arg-AMC substrate concentrations from 0.2–25 μM, in the presence of increasing concentrations of nicotinamide (0–50 mM). The pattern of a Lineweaver-Burk double reciprocal plot of the data was consistent with nicotinamide being a non-competitive inhibitor of TbCatB with a K_i of 21.24 ± 0.89 mM (Fig. 4*F*).

Nicotinamide Treatment and Cell Death Markers in Bloodstream Trypanosomes—The effect of nicotinamide on a series of metabolic and cellular parameters was investigated to provide an insight into the nature of the trypanocidal activity of nicotinamide. First, the flow cytometry analysis revealed that the number of dead cells ($SubG_1$) present in the total population increased progressively with time and represented ~50% at 24 h and virtually all the cells after 72 h (Fig. 5*A*).

Glycolysis is the sole source of energy production in bloodstream trypanosomes. We investigated whether the cell death induced by nicotinamide was also due to an inhibitory effect on glycolysis. For this purpose, pyruvate production was quantified by monitoring the kinetics of NADH oxidation produced during pyruvate efflux. No changes in pyruvate efflux rate was

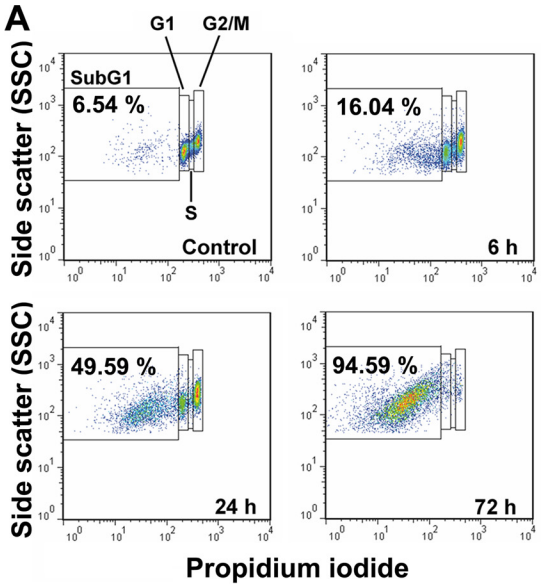

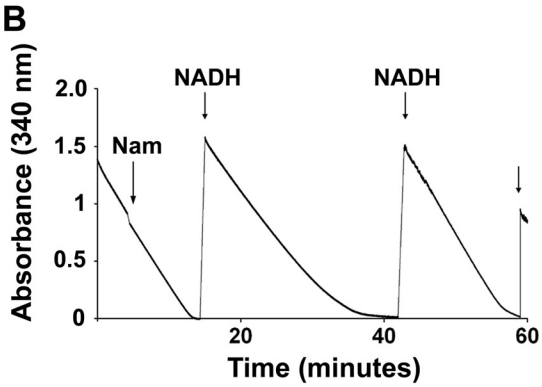

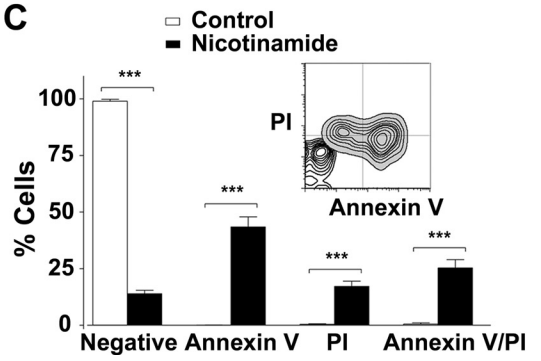

FIGURE 5. **Nicotinamide causes cell death in *T. brucei*.** *A*, representative dot plots from FACS analysis to quantify the dead cell population ($SubG_1$) after nicotinamide treatment. Percentages of the $SubG_1$ population are the mean ± S.E. from three different experiments. *B*, pyruvate efflux measurement. Pyruvate production was quantified by monitoring the kinetics of NADH oxidation (absorbance at 340 nm). *Nam*, nicotinamide. *C*, FACS analysis of bloodstream forms stained with annexin V-FITC and PI. *Error bars* represent mean ± S.D. from three independent experiments. The percentages were determined using CellQuest software. Statistical significance was determined by Bonferroni's multiples comparison test between treated *versus* untreated cells. ***, $p < 0.0001$. A representative overlay dot plot to compare the different populations between treated and untreated trypanosomes was performed with FlowJo software.

observed after nicotinamide addition, indicating that glycolysis was not inhibited (Fig. 5*B*).

Finally, the surface appearance of phosphatidyl serine was also analyzed by annexin V/PI double-staining protocol (Fig. 5*C*). Bloodstream trypanosomes were incubated for 24 h with nicotinamide, and then phosphatidyl serine exposure was quantified by flow cytometry. After 24 h of incubation with nicotinamide, almost half the cells (44%) were annexin V-positive but PI-negative and, thus, represented an early apoptotic stage (Fig. 5*C*). In addition, ~25% of the cells were annexin V-positive/PI-positive (late apoptotic) and 17.2% (S.D.± 2.26) annexin V-negative/PI-positive (early necrotic) (Fig. 5*C*). As expected, the total percentage of dead cells, given by the total % PI-positive cells (~43%), correlated with ~50% of the $subG_1$ cell population after 24 h of incubation with nicotinamide (Fig. 5, *A* and *C*). Altogether, these results suggest that cell death induced by nicotinamide treatment in bloodstream trypanosomes shares some biochemical characteristics of programmed cell death in mammalian cells.

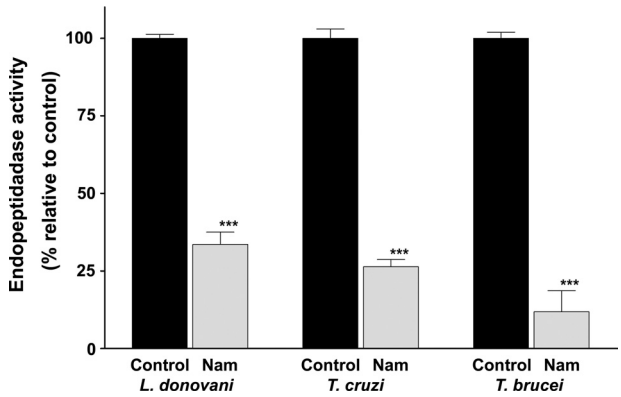

FIGURE 6. **Cathepsin b-like activity in total extracts from *L. donovani*, *T. cruzi*, and *T. brucei*.** Protease activity was measured using the fluorogenic peptide substrate Z-Arg-Arg-AMC after 30 min of incubation in the presence of nicotinamide (*Nam*). Values were normalized to the activity of the control (100%). Data are mean ± S.D. from three different experiments. Statistical significance was determined by Bonferroni's multiple comparison test. ***, $p < 0.001$.

DICUSSION

There is extensive literature describing the antimicrobial activity of nicotinamide against a range of pathogens such as bacteria, parasite protozoa (including trypanosomatids), fungi, and viruses (10–15, 36), but the basis for this activity remains largely unknown. This study provides new insights into the anti-trypanosome activity of nicotinamide by characterizing the nature and kinetics of the pathological process and by identifying the inhibition of a specific and essential target in trypanosomes. Together, the findings support the view that incubation with nicotinamide causes deleterious defects in the endocytic traffic, disruption of the lysosome, a failure of cytokinesis, and, ultimately, cell death. Furthermore, these effects can be attributed to the rapid inhibition of a cathepsin b-like activity that previous studies have shown to be essential in *T. brucei*. Moreover, an assay of purified recombinant TbCatB demonstrated directly that nicotinamide inhibits this activity with the characteristics of a non-competitive inhibitor with a K_i of 21.24 ± 0.89 mM. Nicotinamide also inhibited cysteine protease activity in total extracts from *T. cruzi* and *L. donovani* (Fig. 6). This result suggests that inhibition of a cathepsin b protease may also be the reason why nicotinamide is toxic to these parasites.

The effects of nicotinamide on parasite morphology, as revealed by light and electron microscopy, were all consistent with a defect in endocytic traffic, leading to an enlargement of the flagellar pocket. This inhibitory effect on endocytic traffic was confirmed by a decreased uptake of FITC-labeled tomato lectin observed in the presence of nicotinamide, whereas the disruptive effect on the location of the lysosomal membrane protein p67 suggested a perturbation of the lysosome under these conditions. Overall, these effects were similar to those observed following treatment with well characterized cysteine protease inhibitors and, more significantly, were also observed following knockdown of a cathepsin b-like activity in trypanosomes (21). However, in the case of knockdown cells, these effects take longer to appear, presumably because reduction of the protease activity below permissive levels reflects normal turnover of the protein. In contrast, inhibition of protease activity by nicotinamide is very fast, as total cellular activity decreases by 75% within 1 min of addition of the inhibitor to cell lysates. The residual protease activity decreased only marginally, which may indicate a nicotinamide-insensitive component in the total cellular protease activity. Thus, protease inhibition is likely to be the first effect of incubation with nicotinamide, followed by effects on endocytosis, transferrin degradation, and morphological effects, which are visible after 3 h. Assay of transferrin uptake demonstrated that the cell associated fluorescence increases rapidly during the first 5 min before falling to and being maintained at a relatively constant level for the next 30 min in control cells. This result fits with the fact that receptor-mediated endocytosis in bloodstream forms is characterized by a rapid uptake of the ligand, followed by subsequent proteolytic digestion and excretion of the breakdown products. Thus, the steady-state level of cell-associated fluorescence reflects a balance between the continuous uptake, breakdown, and excretion pathways. However, after preincubation with nicotinamide, *i.e.* following a major loss of protease activity, uptake of transferrin was lower than in control cells. But eventually, intracellular transferrin overshot the steady level of the cell-associated label observed in control cells, not reaching a plateau even after 40 min. This finding suggested decreased receptor-mediated endocytosis coupled with an accumulation of nondegraded ligand within the cell. Thus, the effect of nicotinamide on transferrin uptake fits with the view that receptor-mediated uptake of macromolecules from the flagellar pocket is linked to the proper function of endosomal/lysosomal compartments with respect to protease activity and acidic pH and the finding that this traffic is sensitive to protease inhibitors and membrane-permeable weak bases (30, 37, 38).

The morphological effects of nicotinamide are also consistent with the disruption of normal endocytic traffic and agree with the well described enlargement of the flagellar pocket and disruption of the lysosomal/endosomal compartments that occurs when proteins associated with vesicle traffic in bloodstream forms are subjected to RNAi, *e.g.* clathrin and components of the actin cytoskeleton (26, 27, 34). However, the nicotinamide-induced morphological effects are apparent after 3 h, whereas in the case of RNAi cells, typically, inductions of 24 h or more are required for morphological pathologies to present themselves. As expected, the RNAi effect depends on the turnover of the components. Enlargement of the pocket, or the big eye phenotype, is thought to reflect an imbalance between endocytic traffic from the pocket and the continuous export of new membrane and proteins to the surface via the pocket. This export traffic probably reflects the fact that trypanosomes continue to engage in mitosis and re-enter the cell cycle but fail to undergo cytokinesis under these conditions. Analysis of the cellular DNA content and kinetoplast/nucleus ratio demonstrated that nicotinamide treatment caused a cell cycle arrest at G_2 phase and a blockage of cytokinesis, and the same effect was observed in TbCatB RNAi cells (21). A failure of cytokinesis but not mitosis appears as a common outcome of the knockdown of many essential proteins in bloodstream forms of *T. brucei* and can have multiple origins (39). Clearly, inhibition of cathepsin b-like activity, either by RNAi or incubation with nicotinamide, causes a blockage in endocytosis that leads to disruption in vesicle traffic which ultimately leads to a failure in cytokinesis and eventually cell death. It is unclear precisely how inhibition of a soluble protease in lysosomal/endosomal compartments can affect the endocytic machinery located in the cytoplasm, but it presumably reflects an accumulation of non-degraded macromolecules and loss of the ability to sort receptors and cargo. Interestingly, treatment with nicotinamide caused an increase in the accumulation of the LysoTracker dye, indicating that there is an increase in the number of intracellular acidic organelles. This effect might be due to a general defect in vesicle trafficking/sorting, perhaps in an attempt to overcome the inhibition in protein degradation.

Finally, nicotinamide is particularly cheap to produce, distribute, and deliver to humans. It can be administered orally and cross the blood brain barrier. Thus, nicotinamide may be a valuable and rational candidate as a lead compound for anti-trypanosomal drug development. Such compounds may provide a new class of anti-trypanosomal drugs specifically interfering with the iron metabolism of the parasite.

Acknowledgments—We thank Derek Nolan (Trinity College Dublin, Dublin, Ireland) and Luis Rivas (Centro de Investigaciones Biológicas, Consejo Superior de Investigaciones Científicas, Madrid, Spain) for valuable input on TbCatB kinetics studies and for critical reading of the manuscript. We also thank Estela Pineda-Molina and Sonia Ibáñez (Factoría Española de Cristalización, Consolider-Ingenio 2010, Ministerio de Ciencia e Innovación, Spain), Santiago Castanys, Francisco Gamarro, and José M Pérez-Victoria (Instituto de Parasitología y Biomedicina López-Neyra, Consejo Superior de Investigaciones Científicas, IPBLN-CSIC, Granada, Spain) for technical support; Jay Bangs (University of Wisconsin-Madison, Madison, WI) for p67 antibodies; Conor Caffrey, Jim McKerrow (University of California, San Francisco, CA), and Zachary Mackey (Virginia Polytechnic Institute and State University, Blacksburg, VA) for TbCatB plasmids; Elena González-Rey (IPBLN-CSIC, Granada, Spain) for the HUVEC cell line; José Luis García-Pérez (Centro Pfizer-Universidad de Granada-Junta de Andalucía de Genómica e Investigación Oncológica, Granada, Spain) for human foreskin fibroblast cells; D. Porcel-Muñoz, and J. D. Bueno-Pérez (Scientific Instrumentation Center of the University of Granada, Granada, Spain) for providing electron microscopy analysis; and our colleagues Teresa del Castillo and Carlos Rodrigues-Poveda for helpful discussions.

REFERENCES

1. Liu, G., Foster, J., Manlapaz-Ramos, P., and Olivera, B. M. (1982) Nucleoside salvage pathway for NAD biosynthesis in *Salmonella typhimurium*. *J. Bacteriol.* **152,** 1111–1116
2. Jackson, T. M., Rawling, J. M., Roebuck, B. D., and Kirkland, J. B. (1995) Large supplements of nicotinic acid and nicotinamide increase tissue NAD+ and poly(ADP-ribose) levels but do not affect diethylnitrosamine-induced altered hepatic foci in Fischer-344 rats. *J. Nutr.* **125,** 1455–1461
3. Sakai, Y., Jiang, J., Kojima, N., Kinoshita, T., and Miyajima, A. (2002) Enhanced *in vitro* maturation of fetal mouse liver cells with oncostatin M, nicotinamide, and dimethyl sulfoxide. *Cell. Transplant.* **11,** 435–441
4. Vaca, P., Berná, G., Martín, F., and Soria, B. (2003) Nicotinamide induces both proliferation and differentiation of embryonic stem cells into insulin-producing cells. *Transplant. Proc.* **35,** 2021–2023
5. Sun, A. Y., and Cheng, J. S. (1998) Neuroprotective effects of poly (ADP-ribose) polymerase inhibitors in transient focal cerebral ischemia of rats. *Zhongguo Yao Li Xue Bao* **19,** 104–108
6. Mokudai, T., Ayoub, I. A., Sakakibara, Y., Lee, E. J., Ogilvy, C. S., and Maynard, K. I. (2000) Delayed treatment with nicotinamide (Vitamin B(3)) improves neurological outcome and reduces infarct volume after transient focal cerebral ischemia in Wistar rats. *Stroke* **31,** 1679–1685
7. Klaidman, L., Morales, M., Kem, S., Yang, J., Chang, M. L., and Adams, J. D., Jr. (2003) Nicotinamide offers multiple protective mechanisms in stroke as a precursor for NAD+, as a PARP inhibitor and by partial restoration of mitochondrial function. *Pharmacology* **69,** 150–157
8. Kallmann, B., Burkart, V., Kröncke, K. D., Kolb-Bachofen, V., and Kolb, H. (1992) Toxicity of chemically generated nitric oxide towards pancreatic islet cells can be prevented by nicotinamide. *Life Sci.* **51,** 671–678
9. Maiese, K., Chong, Z. Z., Hou, J., and Shang, Y. C. (2009) The vitamin nicotinamide. Translating nutrition into clinical care. *Molecules* **14,** 3446–3485
10. Murray, M. F. (2003) Nicotinamide. An oral antimicrobial agent with activity against both *Mycobacterium tuberculosis* and human immunodeficiency virus. *Clin. Infect. Dis.* **36,** 453–460
11. Sereno, D., Alegre, A. M., Silvestre, R., Vergnes, B., and Ouaissi, A. (2005) *In vitro* antileishmanial activity of nicotinamide. *Antimicrob. Agents Chemother.* **49,** 808–812
12. Gazanion, E., Vergnes, B., Seveno, M., Garcia, D., Oury, B., Ait-Oudhia, K., Ouaissi, A., and Sereno, D. (2011) *In vitro* activity of nicotinamide/antileishmanial drug combinations. *Parasitol. Int.* **60,** 19–24
13. Prusty, D., Mehra, P., Srivastava, S., Shivange, A. V., Gupta, A., Roy, N., and Dhar, S. K. (2008) Nicotinamide inhibits *Plasmodium falciparum* Sir2 activity *in vitro* and parasite growth. *FEMS Microbiol. Lett.* **282,** 266–272
14. Soares, M. B., Silva, C. V., Bastos, T. M., Guimarães, E. T., Figueira, C. P., Smirlis, D., and Azevedo, W. F., Jr. (2012) Anti-*Trypanosoma cruzi* activity of nicotinamide. *Acta Trop.* **122,** 224–229
15. Murray, M. F., and Srinivasan, A. (1995) Nicotinamide inhibits HIV-1 in both acute and chronic *in vitro* infection. *Biochem. Biophys. Res. Commun.* **210,** 954–959
16. (1986) Epidemiology and control of African trypanosomiasis. Report of a WHO Expert Committee. *World Health Organ. Tech. Rep. Ser.* **739,** 1–127
17. McKerrow, J. H., Caffrey, C., Kelly, B., Loke, P., and Sajid, M. (2006) Proteases in parasitic diseases. *Annu. Rev. Pathol.* **1,** 497–536
18. Vermelho AB, G.-d.-S. S., d'Avila-Levy CM, et al. (2007) Trypanosomatidae peptidases. A target for drugs development. *Curr. Enzyme. Inhib.* **3,** 19–48
19. Scory, S., Caffrey, C. R., Stierhof, Y. D., Ruppel, A., and Steverding, D. (1999) *Trypanosoma brucei*. Killing of bloodstream forms *in vitro* and *in vivo* by the cysteine proteinase inhibitor Z-Phe-Ala-CHN2. *Exp. Parasitol.* **91,** 327–333
20. Scory, S., Stierhof, Y. D., Caffrey, C. R., and Steverding, D. (2007) The cysteine proteinase inhibitor Z-Phe-Ala-CHN2 alters cell morphology and cell division activity of *Trypanosoma brucei* bloodstream forms *in vivo*. *Kinetoplastid Biol. Dis.* **6,** 2
21. Mackey, Z. B., O'Brien, T. C., Greenbaum, D. C., Blank, R. B., and McKerrow, J. H. (2004) A cathepsin B-like protease is required for host protein degradation in *Trypanosoma brucei*. *J. Biol. Chem.* **279,** 48426–48433
22. Abdulla, M. H., O'Brien, T., Mackey, Z. B., Sajid, M., Grab, D. J., and McKerrow, J. H. (2008) RNA interference of *Trypanosoma brucei* cathepsin B and L affects disease progression in a mouse model. *PLoS Negl. Trop. Dis.* **2,** e298
23. Räz, B., Iten, M., Grether-Bühler, Y., Kaminsky, R., and Brun, R. (1997) The Alamar Blue assay to determine drug sensitivity of African trypanosomes (*T. b. rhodesiense* and *T. b. gambiense*) *in vitro*. *Acta Trop.* **68,** 139–147
24. Gould, M. K., Vu, X. L., Seebeck, T., and de Koning, H. P. (2008) Propidium iodide-based methods for monitoring drug action in the kinetoplastidae. Comparison with the Alamar Blue assay. *Anal. Biochem.* **382,** 87–93
25. Nicoletti, I., Migliorati, G., Pagliacci, M. C., Grignani, F., and Riccardi, C. (1991) A rapid and simple method for measuring thymocyte apoptosis by propidium iodide staining and flow cytometry. *J. Immunol. Methods* **139,** 271–279
26. García-Salcedo, J. A., Pérez-Morga, D., Gijón, P., Dilbeck, V., Pays, E., and Nolan, D. P. (2004) A differential role for actin during the life cycle of *Trypanosoma brucei*. *EMBO J.* **23,** 780–789
27. Spitznagel, D., O'Rourke, J. F., Leddy, N., Hanrahan, O., and Nolan, D. P. (2010) Identification and characterization of an unusual class I myosin involved in vesicle traffic in *Trypanosoma brucei*. *PLoS ONE* **5,** e12282
28. Landeira, D., and Navarro, M. (2007) Nuclear repositioning of the VSG promoter during developmental silencing in *Trypanosoma brucei*. *J. Cell. Biol.* **176,** 133–139
29. Caffrey, C. R., Hansell, E., Lucas, K. D., Brinen, L. S., Alvarez Hernandez, A., Cheng, J., Gwaltney, S. L., 2nd, Roush, W. R., Stierhof, Y. D., Bogyo, M., Steverding, D., and McKerrow, J. H. (2001) Active site mapping, biochemical properties and subcellular localization of rhodesain, the major cysteine protease of *Trypanosoma brucei* rhodesiense. *Mol. Biochem. Parasitol.* **118,** 61–73
30. O'Brien, T. C., Mackey, Z. B., Fetter, R. D., Choe, Y., O'Donoghue, A. J., Zhou, M., Craik, C. S., Caffrey, C. R., and McKerrow, J. H. (2008) A parasite cysteine protease is key to host protein degradation and iron acquisition. *J. Biol. Chem.* **283,** 28934–28943
31. Mendoza-Palomares, C., Biteau, N., Giroud, C., Coustou, V., Coetzer, T., Authié, E., Boulangé, A., and Baltz, T. (2008) Molecular and biochemical characterization of a cathepsin B-like protease family unique to *Trypanosoma congolense*. *Eukaryot. Cell.* **7,** 684–697
32. Lim, C. S., Potts, M., and Helm, R. F. (2006) Nicotinamide extends the replicative life span of primary human cells. *Mech. Ageing Dev.* **127,** 511–514
33. Kang, H. T., Lee, H. I., and Hwang, E. S. (2006) Nicotinamide extends replicative lifespan of human cells. *Aging Cell.* **5,** 423–436
34. Allen, C. L., Goulding, D., and Field, M. C. (2003) Clathrin-mediated endocytosis is essential in *Trypanosoma brucei*. *EMBO J.* **22,** 4991–5002
35. Kelley, R. J., Alexander, D. L., Cowan, C., Balber, A. E., and Bangs, J. D. (1999) Molecular cloning of p67, a lysosomal membrane glycoprotein from *Trypanosoma brucei*. *Mol. Biochem. Parasitol.* **98,** 17–28
36. Wurtele, H., Tsao, S., Lépine, G., Mullick, A., Tremblay, J., Drogaris, P., Lee, E. H., Thibault, P., Verreault, A., and Raymond, M. (2010) Modulation of histone H3 lysine 56 acetylation as an antifungal therapeutic strategy. *Nat. Med.* **16,** 774–780
37. Mellman, I., Fuchs, R., and Helenius, A. (1986) Acidification of the endocytic and exocytic pathways. *Annu. Rev. Biochem.* **55,** 663–700
38. Coppens, I., Baudhuin, P., Opperdoes, F. R., and Courtoy, P. J. (1993) Role of acidic compartments in *Trypanosoma brucei*, with special reference to low-density lipoprotein processing. *Mol. Biochem. Parasitol.* **58,** 223–232
39. Hammarton, T. C. (2007) Cell cycle regulation in *Trypanosoma brucei*. *Mol. Biochem. Parasitol.* **153,** 1–8